




Article

Assessing the Accuracy of 50 Temperature-Based Models for Estimating Potential Evapotranspiration (PET) in a Mediterranean Mountainous Forest Environment

Nikolaos D. Proutsos ^{1,*} , Mariangela N. Fotelli ², Stefanos P. Stefanidis ²  and Dimitris Tigkas ³ 

¹ Institute of Mediterranean Forest Ecosystems, Hellenic Agricultural Organization—DIMITRA, Terma Alkmanos, 11528 Athens, Greece

² Forest Research Institute, Hellenic Agricultural Organization—DIMITRA, Vassilika, 57006 Thessaloniki, Greece; fotelli@elgo.gr (M.N.F.); sstefanidis@elgo.gr (S.P.S.)

³ Centre for the Assessment of Natural Hazards and Proactive Planning & Laboratory of Reclamation Works and Water Resources Management, National Technical University of Athens, 15780 Athens, Greece; ditigas@mail.ntua.gr

* Correspondence: np@fria.gr

Abstract: Potential evapotranspiration (PET) is a crucial parameter for forest development, having an important role in ecological, biometeorological, and hydrological assessments. Accurate estimations of PET using the FAO–56 Penman–Monteith (FAO–56 PM) benchmark method require a wide range of data parameters, which are not typically available at meteorological stations installed in forest environments. The aim of this study is to investigate the accuracy of various methods with low data requirements for assessing PET in a Mediterranean forest environment and propose appropriate alternatives for accurate PET estimation. Specifically, 50 temperature-based methods were evaluated against the FAO–56 PM method in a sub-humid forest in northern Greece, using high-quality daily meteorological data. The outcomes indicate that temperature-based methods offer a viable alternative for PET estimation when data availability is limited, with a considerable number of methods (22) presenting low deviations (up to 10%) compared to the benchmark method. Temperature-based models outperformed those incorporating water-related parameters (as relative humidity or precipitation) in Mediterranean forest environments. The top performing methods in the study site, based on several statistical indices, were the equations of Ravazzani et al., proposed in 2012, followed by Hargreaves–Samani in 1985 and Heydari and Heydari in 2014.

Keywords: forest micrometeorology; evapotranspiration; Mediterranean conditions; mountainous sites; vegetation water requirements; water cycle



Citation: Proutsos, N.D.; Fotelli, M.N.; Stefanidis, S.P.; Tigkas, D. Assessing the Accuracy of 50 Temperature-Based Models for Estimating Potential Evapotranspiration (PET) in a Mediterranean Mountainous Forest Environment. *Atmosphere* **2024**, *15*, 662. <https://doi.org/10.3390/atmos15060662>

Academic Editor: Sonia Wharton

Received: 14 May 2024

Revised: 27 May 2024

Accepted: 30 May 2024

Published: 30 May 2024



Copyright: © 2024 by the authors. Licensee MDPI, Basel, Switzerland. This article is an open access article distributed under the terms and conditions of the Creative Commons Attribution (CC BY) license (<https://creativecommons.org/licenses/by/4.0/>).

1. Introduction

Evapotranspiration (ET) is an essential part of the water cycle and plays a key role in several disciplines of geosciences, including climate classification and drought assessment, hydrological modeling, irrigation planning, water resources management, ecosystems' adaptation to climate change, and accounting for ecosystem services [1–9]. Thus, accurate estimates of ET are necessary for implementing water management strategies and promoting efficient use of water resources, especially in regions facing water shortage, like the Mediterranean basin. Unfortunately, direct measurements of ET through techniques like lysimeters [10,11], eddy covariance [12,13], and the Bowen ratio energy balance (BREB) system are difficult due to the expensive equipment required and the practical difficulties involved. Therefore, several empirical mathematical models have been developed worldwide under various environments to estimate ET using meteorological data. Various models possess specific strengths and limitations, which are dependent on the methods' applications and underlying assumptions [14]. In all these models, it is of paramount

importance to note that the magnitude of ET is significantly influenced by the surface characteristics of the site [15].

The empirical ET models aim to provide reliable estimations of water demand solely driven by atmospheric conditions, regardless of crop or vegetation characteristics and soil factors. As a result, the output of these models is referred to as potential (PET) or reference evapotranspiration, which are different terms with different conceptual and physical bases for expressing water demand [16,17]. PET models can be classified into four major groups: mass-transfer, temperature-based, radiation-based, and combination methods. It is noteworthy that selection of the appropriate PET method for each specific site is of the utmost importance due to its impact on the computation of hydro-meteorological and climatic indices that are widely used for environmental monitoring [8,18–20].

The Food and Agriculture Organization of the United Nations (FAO) and the World Meteorological Organization (WMO) recommend the standardized FAO56 Penman–Monteith (FAO56–PM) equation for PET estimation [21]. The FAO56–PM equation is known for its accuracy across various climates and time periods [22] and serves as a standard for comparing other empirical or soft computing methods in most studies [23,24]. The advantage of this method lies in its ability to bypass the need for local calibration, as it encompasses both physiological and aerodynamic parameters. Moreover, the equation has undergone rigorous testing, making use of lysimeter data to validate its accuracy and reliability [25]. On the other hand, its application is not always feasible due to high data requirements, such as air temperature, relative humidity, wind speed, and solar radiation data, which are available in limited meteorological stations worldwide. Additionally, obtaining quality data from these parameters can also be challenging [26].

Thus, it is crucial to develop models that strike a balance between accuracy and simplicity, utilizing fewer meteorological parameters to allow more straightforward estimates of PET compared to the FAO56–PM method. Moreover, the adjustment or calibration of simpler original methods with reduced data requirements becomes essential to accurately estimate PET, particularly in regions where meteorological data are scarce [27].

In this context, several studies have evaluated the performance of PET methods against the FAO56–PM, considering a limited number of methods at a time [28–35], and conducted in low-humidity conditions at low altitudes, exclusively for urban and agricultural areas. In contrast, a recent thorough evaluation of 127 PET models was performed in two Mediterranean urban green sites [23]. Overall, previous studies conclude that combination-based methods (which are equally demanding with FAO56–PM) performed best for PET estimation, followed by radiation-based and temperature-based ones, whilst less accurate results are given by the mass-transfer-based method.

The temporal variability of PET is important especially for rainfed forest environments [36–38]. Exploring the performance of PET methods in forest ecosystems is particularly important for understanding water interactions and balance in forest ecosystems, as well as for assessing the water requirements and growth of forest vegetation [39,40]. Moreover, it becomes essential to assess model performance at high altitudes, where PET values exhibit distinctively higher levels, and models might display varying uncertainties. However, there is limited comparative evaluation of empirical PET models in forest ecosystems. This is due to the challenges associated with installing and maintaining meteorological stations at high elevations in mountainous regions. The most notable studies are analyzed below. Federer et al. [41] compared five reference surface PET methods to four surface-dependent PET methods in different forest types at seven locations. Another study, conducted at a coniferous forest site in northern California [42] compared five models and proposed a modified Priestley–Taylor model. Rao et al. [43] compared the estimates of three PET models with measured actual ET in two forested watersheds (Appalachian Mountains, North America), with one dominated by a conifer plantation and one dominated by native naturally regenerated deciduous hardwoods. Ha et al. [44] compared five PET models with ET measurements with the eddy covariance method in three ponderosa pine forests in Arizona. In Greece, Gebhart et al. [45] evaluated the performance of 13 PET methods

against FAO56–PM in forest sites of northern Greece. Bourletsikas et al. [46] published a comparative evaluation of 24 PET equations applied on an evergreen-broadleaved forest in central Greece. More recently, Markos and Radoglou (2021) conducted a study comparing FAO56–PM PET values with eddy covariance measurements from a *Robinia pseudoacacia* site in northern Greece.

Understanding the behavior of PET models in such environments is crucial for ensuring accurate estimations and reliable predictions in specific climatic conditions. Hence, conducting evaluations in high-altitude regions can lead to valuable insights and improve the overall reliability of PET models in challenging terrains. Therefore, thorough evaluation of a wide range of PET methods in forest environments is of high importance.

This study follows the work by Proutsos et al. [23] who evaluated the performance of empirical PET methods in urban green spaces in Greece. The present study aims at investigating the performance of 50 temperature-based PET methods against the benchmark FAO56–PM method, in a mountainous forest site in northern Greece, to evaluate the applicability of methods with limited data requirements in the Mediterranean forest environment. Daily data from an automatic forest meteorological station were employed to produce the PET estimates for 5389 days over the period from 2008 to 2023. The findings of this work can contribute to improving our understanding of water dynamics in forest ecosystems and provide valuable tools for assessing forest vegetation water requirements and growth under specific climatic and geographical conditions.

Based on the previous work by Proutsos et al. [23] in urban green spaces in Greece, the present study aims at investigating the performance of 50 temperature-based PET methods against the benchmark FAO56–PM method, in a mountainous forest site in northern Greece. Daily data from an automatic forest meteorological station were employed to produce the PET estimates for 5389 days over the period from 2008 to 2023. The results can contribute to improving our understanding of water dynamics in forest ecosystems and provide valuable tools for assessing forest vegetation water requirements and growth under specific climatic and geographical conditions. In addition, the evaluation of low-demand temperature-based PET methods can support the applicability of the appropriate methods in mountainous Mediterranean forest environments with limited data availability.

2. Materials and Methods

2.1. Study Site

The study site is located in the area of Chrysopigi village (Figure 1), about 13 km northeast from the Serres Municipality. The forest meteorological station was installed at 605m a.s.l., at the Research Center of the Forest Research Institute (41°10' N, 23°34' E) in 1978. In 2008, the station was upgraded to automatic and monitoring of radiation fluxes was added.

Based on the long-term meteorological data of the 45-year period from 1978 to 2023 from the same station, the climate of the region is characterized by an average annual air temperature of 13.3 °C (with a standard deviation SD = 0.7) ranging seasonally from 4.4 °C (SD = 1.2) in winter to 22.8 °C (SD = 1.0) in summer, with intermediate values at the transitional seasons of spring (12.0 °C, SD = 1.2) and autumn (14.2 °C, SD = 1.1). The warmest month of the year is August (23.6 °C, SD = 1.5) and the coolest is January (3.6 °C, SD = 1.7). The annual precipitation in Chrysopigi is 623 mm, almost uniformly distributed between seasons (27% in winter, 27% in spring, 22% in summer, and 24% in autumn), which is not typical of the Mediterranean climate of Greece which is characterized by wet winters and dry summers.

The above patterns result in the classification of the area in the sub-humid climatic type with very cold winters, according to Emberger's [47] bioclimatic classification, with a Q_2 index of 77.0. The dry summer conditions last about 2 months (from the beginning of July to the end of August) as depicted in the Bagnouls and Gausson [48] pluviometric diagram of the area (Figure 2).

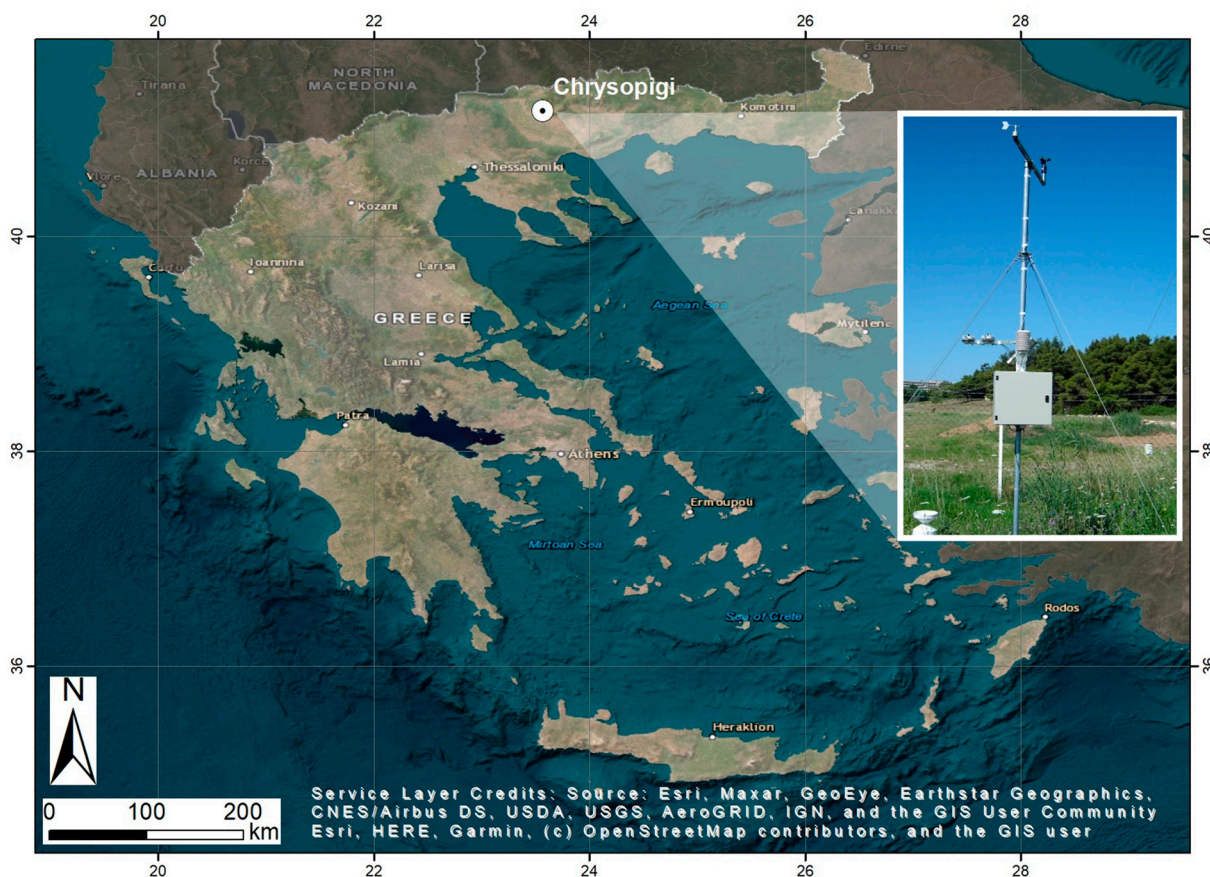


Figure 1. Map of Greece, where the study site of Chrysopigi is indicated.

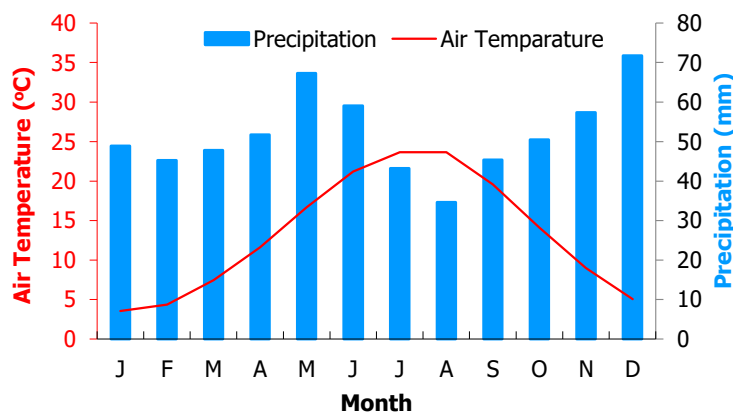


Figure 2. Pluviometric diagram of Chrysopigi, produced by long-term data (period 1978–2023).

The broader area belongs to the *Quercetalia pubescentis* vegetation zone with the presence of *Quercus pubescens*, *Q. coccifera*, *Caprinus orientalis*, *Fraxinus ornus*, *Cistus incanus*, and *Colutea arborescens*. Its larger part is occupied by a 60-year-old planted *Pinus brutia* forest. Kermes oak (*Q. coccifera*) dominates especially in the forest openings [49]. The soil is, generally, sandy loam, with shallow depth and pH of about 6 and organic matter content of 1.47% [49].

In a forest opening, a fully equipped meteorological station recorded data on a 60 min timestep. Air temperature and relative humidity (E+E sensor, model EE08; E+E Elektronik Ges.m.b.H., Engerwitzdorf, Austria, with accuracy less than ±3% for relative humidity and less than 0.2 °C at 23 °C), windspeed (Thies Clima Small Wind transmitter, Adolf Thies GmbH & Co. KG, Göttingen, Germany, with accuracy ±0.5 m s⁻¹) and wind direction

(NRG 200P; Kintech Engineering, Zaragoza, Spain), precipitation PR (Pronamic ApS rain gauge; Skjern, Denmark, with accuracy ±2%), and global solar radiation (SP110 Apogee Pyranometer; Apogee Instruments Inc., Logan, UT, USA, with typical absolute calibration error of less than 3% ± 5% cosine error) were measured with a Symmetron Stylitis–10 datalogger (Symmetron Electronic Applications, Gerakas, Athens, Greece).

Meteorological data of the period from January 2008 to May 2023 were employed to produce estimates of potential daily evapotranspiration (PET) by different empirical models. Specifically, air temperature T and relative humidity RH (average, minimum, and maximum), precipitation, wind speed, and global solar radiation daily values were used to produce the daily PET values. The analysis was performed on the PET estimates. A total number of 5389 daily values were assessed based on the PET estimates with the FAO56 Penman Monteith (FAO56–PM). The values are almost evenly distributed among seasons: 26% in winter, 26% in spring, 24% in summer, and 24% in autumn.

2.2. Potential Evapotranspiration Empirical Models Temperature-Based Potential Evapotranspiration (PET) Methods

In this study several temperature-based empirical models were applied to estimate PET. In general, the models can be grouped into three main categories based on the data input requirements. The two groups of equations, along with the mathematical expression for each equation, are presented below.

- PET = f (T), 36 methods presented in Equations (1)–(36) in Table 1.
- PET = f (T, RH), 13 methods presented in Equations (37)–(49) in Table 2.
- PET = f (T, PR), 1 method presented in Equation (50) in Table 2.

Table 1. Temperature-based methods. General form PET = f (T).

Method	Equation PET = f(T) *	Equation No	References
Thornthwaite 1948	$PET = 16 \left(\frac{10T}{I} \right)^a \frac{N}{360}$	(1)	[50,51]
Blaney & Criddle 1950	$PET = \begin{cases} 0.85 p (0.46 t + 8.13), & \text{from April to September} \\ 0.45 p (0.46 t + 8.13), & \text{from October to March} \end{cases}$	(2)	[52]
McCloud 1955	$PET = 0.254 \cdot 1.07^{1.8 T}$	(3)	[53]
Hamon 1963	$PET = 29.8 N \left(\frac{e_s}{T+273.2} \right)$ for T > 0	(4)	[54,55]
Baier & Robertson 1965	$PET = 0.157 T_{max} + 0.158 (T_{max} - T_{min}) + 0.109 R_a - 5.39$	(5)	[56]
Malmstrom 1969	$PET = 40.9 e_s \frac{N}{360}$	(6)	[54]
Siebert & Schrödter 1975	$PET = 0.533 \left(\frac{10T}{33.617} \right)^{1.033} \frac{N}{12}$	(7)	[57]
Blaney & Criddle (Mid. Eur. Ver.)	$PET = -1.55 + 0.96 p (0.457 T + 8.128)$	(8)	[16]
Smith & Stopp 1978	$PET = 0.16 T$	(9)	[58]
Hargreaves & Samani 1985	$PET = 0.0023 (T_{max} - T_{min})^{0.5} (T + 17.8) R_a$	(10)	[59]
Kharrufa 1985	$PET = 0.34 p T^{1.3}$	(11)	[60]
Mintz & Walker 1993	$PET = 0.17 \frac{N}{12} T$	(12)	[61]
Camargo et al., 1999	$PET = 16 \left(\frac{10 T_{ef}}{I} \right)^a \frac{N}{360}, T_{ef} = 0.36(3T_{max} - T_{min})$	(13)	[62]
Samani 2000	$PET = 0.0135 KT R_a (T_{max} - T_{min})^{0.5} (T + 17.8)$ $KT = 0.00185 (T_{max} - T_{min})^2 - 0.0433 (T_{max} - T_{min}) + 0.4023$	(14)	[59,63,64]
Xu & Singh 2001 (1)	$PET = 20 \left(\frac{10T}{I} \right)^a \frac{N}{360}$	(15)	[65]
Xu & Singh 2001 (2)	$PET = 20.5 \left(\frac{10T}{I} \right)^a \frac{N}{360}$	(16)	[65]
Xu & Singh 2001 (3)	$PET = 0.37 p T^{1.3}$	(17)	[65]
Xu & Singh 2001 (4)	$PET = 0.0028 (T_{max} - T_{min})^{0.5} (T + 17.8) R_a$	(18)	[65]
Droogers & Allen 2002 (1)	$PET = 0.0030 (T_{max} - T_{min})^{0.4} (T + 20) R_a$	(19)	[26]
Droogers & Allen 2002 (2)	$PET = 0.0025 (T_{max} - T_{min})^{0.5} (T + 16.8) R_a$	(20)	[26]
Pereira & Pruitt 2004	$PET = 16 \left(\frac{10 T_{ef}^*}{I} \right)^a \frac{N}{360}$ $T_{ef}^* = 0.345(3T_{max} - T_{min}) \frac{N}{24-N}, \text{ for } T \leq T_{ef}^* \leq T_{max}$	(21)	[50]
Trajcovic 2005 (1)	$PET = 0.88 \left[16 \left(\frac{10T}{I} \right)^a \frac{N}{360} \right] + 0.565$	(22)	[66]
Trajcovic 2005 (2)	$PET = 0.817 \left[0.0023 (T_{max} - T_{min})^{0.5} (T + 17.8) R_a \right] + 0.320$	(23)	[66]
Oudin 2005	$PET = R_a \frac{T+5}{100}, \text{ for } T + 5 > 0$	(24)	[67]
Castañeda & Rao 2005 (1)	$PET = \begin{cases} 0.9 p (0.46 T + 8.13), & \text{from April to September} \\ 0.6 p (0.46 T + 8.13), & \text{from October to March} \end{cases}$	(25)	[68]
Trajcovic 2007	$PET = 0.0023 (T_{max} - T_{min})^{0.424} (T + 17.8) R_a$	(26)	[69]

Table 1. Cont.

Method	Equation PET = f(T) *	Equation No	References
Tabari & Talaei 2011 (1)	$PET = 0.0031 (T_{max} - T_{min})^{0.5} (T + 17.8) R_a$	(27)	[27]
Tabari & Talaei 2011 (2)	$PET = 0.0028 (T_{max} - T_{min})^{0.5} (T + 17.8) R_a$	(28)	[27]
Ravazzani et al., 2012	$PET = (0.817 + 0.00022z) 0.0023R_a (T + 17.8)(T_{max} - T_{min})^{0.5}$	(29)	[70]
Berti et al., 2014	$PET = 0.00193 R_a (T + 17.8)(T_{max} - T_{min})^{0.517}$	(30)	[71]
Heydari & Heydari 2014	$PET = 0.0023 (T_{max} - T_{min})^{0.611} (T + 9.519) R_a$	(31)	[72]
Dorji et al., 2016	$PET = 0.002 (T_{max} - T_{min})^{0.296} (T + 33.9) R_a$	(32)	[73]
Lobit et al., 2018	$PET = 0.1555 R_a (0.00428 T + 0.09967) (T_{max} - T_{min})^{0.5}$	(33)	[74]
Althoff et al., 2019	$PET = 0.0135-0.166 R_a (T_{max} - T_{min})^{0.5} (T + 15.3)$	(34)	[75]
Proutsos et al., 2023 Model 3	$PET = 0.026 T^{1.621}$	(35)	[23]
Proutsos et al., 2023 Model 4	$PET = 0.01357 (T + 3.167) (T_{max} - T_{min})^{-0.07} R_a$	(36)	[23]

* where $a = 6.75 \times 10^{-7} I^3 - 7.71 \times 10^{-5} I^2 + 1.7912 \times 10^{-2} I + 0.49239$ and $I = \sum_1^{12} (0.2 T)^{1.514}$ in Equations (1), (13), (15), (16), (21), and (22); p is the daily percentage (%) of annual daytime hours for each day of the year; N are the maximum sunshine daily hours; T, T_{max}, and T_{min} are the daily mean, maximum, and minimum air temperatures in °C; z is the altitude in m; Ra is the extraterrestrial radiation in mm day⁻¹ in all equations, except from Baier & Robertson 1965 (Equation (5)) and Lobit et al. 2018 (Equation (33)), where Ra is in MJ m⁻² d⁻¹; and e_s is the saturation vapor pressure in kPa.

Table 2. Temperature-based methods. General forms PET = f (T, RH) and PET = f (T, PR).

Method	Equation PET = f (T, RH) *	Equation No.	References
Romanenko 1961	$PET = 0.0018 (25 + T)^2 (100 - RH) N / 360$	(37)	[76]
Schendel 1967	$PET = 16 T / RH$	(38)	[77]
Antal 1968	$PET = 0.736 (e_s - e_a)^{0.7} \left(1 + \frac{T}{273}\right)^{4.8}$	(39)	[78,79]
Linacre 1977	$PET = \left[\frac{500(T+0.006z)}{100-\varphi} + 15(T - T_d) \right] / (80 + T)$	(40)	[80]
Xu & Singh 2001 (5)	$PET = 0.0020 (25 + T)^2 (100 - RH) \frac{N}{360}$	(41)	[65]
Xu & Singh 2001 (6)	$PET = \left[\frac{488(T+0.006z)}{100-\varphi} + 15(T - T_d) \right] / (80 + T)$	(42)	[65]
Xu & Singh 2001 (7)	$PET = \left[\frac{615(T+0.006z)}{100-\varphi} + 15(T - T_d) \right] / (80 + T)$	(43)	[65]
Ahooghalaandari et al., 2016 (1)	$PET = 0.252 R_a + 0.221 T \left(1 - \frac{RH}{100}\right)$	(44)	[81]
Ahooghalaandari et al., 2016 (2)	$PET = 0.29 R_a + 0.15 T_{max} \left(1 - \frac{RH}{100}\right)$	(45)	[81]
Ahooghalaandari et al., 2016 (3)	$PET = 0.369 R_a + 0.139 T_{max} \left(1 - \frac{RH}{100}\right) - 1.95$	(46)	[81]
Ahooghalaandari et al., 2016 (4)	$PET = 0.34 R_a + 0.182 T \left(1 - \frac{RH}{100}\right) - 1.55$	(47)	[81]
Proutsos et al., 2023 Model 6	$PET = 0.135 R_a + 0.235 T \left(1 - \frac{RH}{100}\right)$	(48)	[23]
Proutsos et al., 2023 Model 15	$PET = 1.378 (e_s - e_a)^{0.379} \left(1 - \frac{T}{273}\right)^{11.539}$	(49)	[23]

Equation PET = f (T, PR) *			
Droogers & Allen 2002 (3)	$PET = 0.0013 (T_{max} - T_{min} - 0.0123PR)^{0.76} (T + 17) R_a$	(50)	[26]

* where T and T_{max} are the daily mean and maximum air temperatures in °C; T_d is the dewpoint in °C; RH is the relative humidity in %; φ is the latitude in degrees; z is the altitude in m; PR is the monthly precipitation in mm; Ra is the extraterrestrial radiation in mm day⁻¹; and e_s, e_a are the saturation and actual vapor pressures in kPa in all equations, except from Antal 1968 (Equation (39)), where they are in hPa.

The above-presented empirical models were then compared with the benchmark method FAO56-PM [21]:

$$PET = \frac{0.408 \Delta (R_n - G) + \gamma \frac{900}{T+273} u (e_s - e_a)}{\Delta + \gamma(1 + 0.34 u)} \tag{51}$$

2.3. Statistical Indices and Ranking

To compare the estimations of PET by the different models against the estimates by FAO56-PM, the commonly used coefficients of the linear regression $y = ax + b$ were employed as follows: slope a, intercept b, and coefficient of determination R². Four additional statistical measures, recommended by Fox [82], were applied: the mean bias error (MBE) to assess the bias, the variance of the differences distribution s_d² to evaluate the variability of

the differences between the PET values around the MBE, the mean absolute error (MAE), and the root mean square error (RMSE) to express the average difference. The index of agreement (d) was also used to make the cross-comparison between the models [83–85]. The analytic equations for the estimation of the indices are:

$$MBE = \sum_{i=1}^N \frac{P_i - O_i}{N} \tag{52}$$

$$MAE = \sum_{i=1}^N \frac{|P_i - O_i|}{N} \tag{53}$$

$$s_d^2 = \sum_{i=1}^N \frac{(P_i - O_i - MBE)^2}{N - 1} \tag{54}$$

$$RMSE = \sqrt{\sum_{i=1}^N \frac{(P_i - O_i)^2}{N}} \tag{55}$$

$$d = 1 - \frac{\sum_{i=1}^N \frac{(P_i - O_i)^2}{N}}{\sum_{i=1}^N \frac{(|\hat{P}_i| + |\hat{O}_i|)^2}{N}} \tag{56}$$

where O_i is the estimated PET by FAO56-PM, P_i is the PET by the compared methods, $\hat{P}_i = P_i - O$, and $\hat{O}_i = O_i - O$.

To rank the methods, the above indices were used and through a standardization procedure proposed by Aschonitis et al. [86] and also described in Rahimikhoob et al. [87]. The standardized ranking performance index (sRPI) was estimated by the following equations:

$$X_i = \begin{cases} V_i, & \text{Type I indices } (R^2, d) \\ 1 - \frac{|V_i|+1}{|V_{i(max)}|+1}, & \text{Type II indices } (|1 - \text{slope}|, |\text{offset}|, MBE, MAE, s_d^2, RMSE) \end{cases} \tag{57}$$

$$Y_i = \frac{X_i - X_{\min}}{X_{\max} - X_{\min}} \tag{58}$$

$$RPI = \sum_{i=1}^k \frac{Y_i}{k} \tag{59}$$

$$sRPI = \frac{RPI - RPI_{\min}}{RPI_{\max} - RPI_{\min}} \tag{60}$$

where V_i is each statistical index and k is the number of the statistical indices used for the RPI and sRPI estimations.

3. Results

3.1. Meteorological Conditions

For the recording period (1 January 2008 to 16 May 2023), the monthly average patterns of the main meteorological attributes in Chrysopigi are depicted in Figure 3. The average air temperature presented a mean annual value of 13.9 °C, ranging seasonally from 5.2 °C in winter to 23.3 °C in summer. However, there were temperature extremes on the hourly values. The absolute minimum was −11.7 °C, recorded on 8 January 2017, whereas an absolute maximum of 46.8 °C was recorded on 10 June 2015. The annual relative humidity is relatively high (60.6%) with a seasonal variation from 50.7% in summer to 68.8% in winter. The solar radiation pattern, which is the most determinant factor for the formation of PET, follows the distribution of air temperature and presents an annual value of 157 W m^{−2}, being lower in winter (76 W m^{−2}) and maximum in summer (243 W m^{−2}). The sky conditions at the site assessed by the values of atmospheric clearness (Kt, which is defined as the ratio of global solar to extraterrestrial radiation), suggest that at Chrysopigi, intermediate skies generally prevail, with Kt values ranging seasonally from 0.40 in winter to 0.51 in summer.

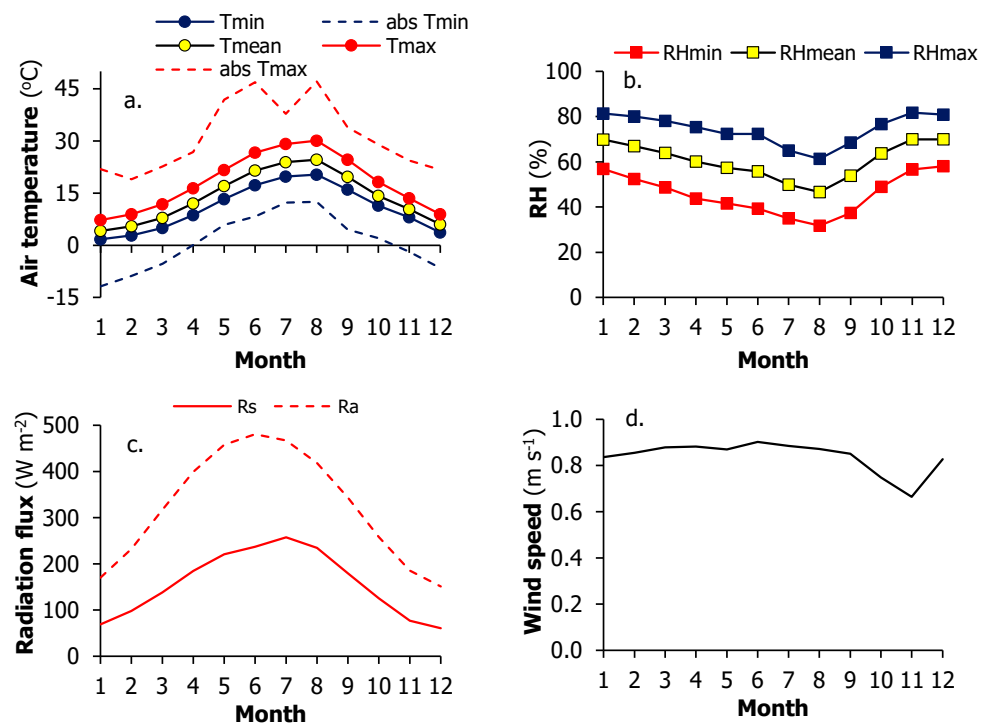


Figure 3. Monthly averages of (a) the mean, T_{mean} , maximum, T_{max} , minimum, T_{min} temperatures, and absolute values of T_{min} and T_{max} ; (b) the mean, RH_{mean} , maximum, RH_{max} , and minimum, RH_{min} relative humidity; (c) the global solar R_s and the extraterrestrial R_a radiation flux densities; and (d) the wind speed, WS , for the site of Chrysopigi in the period 2008–2023.

Under such atmospheric conditions, PET rates by the FAO56–PM model were high in summer (4.43 mm d^{-1}), maximized in July (4.72 mm d^{-1}), and low in winter (0.81 mm d^{-1}), becoming minimum in December (0.63 mm d^{-1}). Moderate rates were estimated for the transitional seasons of spring (2.65 mm d^{-1}) and autumn (1.86 mm d^{-1}), as depicted in Figure 4. The annual average daily PET was 2.44 mm d^{-1} .

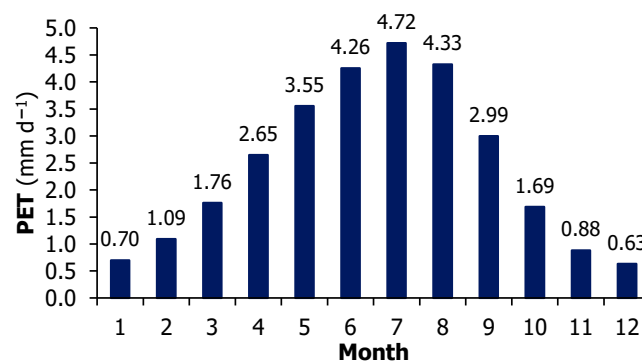


Figure 4. Average monthly values of potential evapotranspiration (PET) estimated by the FAO56–PM benchmark method for the study site of Chrysopigi, for the period 2008–2023.

It is notable that most of the daily data (55.5%) are associated with relatively clear sky conditions (K_t greater than 0.5), whereas about 56.8% of the estimated PET values refer to average daily temperatures less than $15 \text{ }^\circ\text{C}$ (Figure 5). Such a distribution indicates that the PET estimates might be influenced by the local atmospheric clearness conditions and global solar radiation to a high degree. Specifically, the Pearson correlation assessment between the PET estimates by the FAO56–PM and the input parameters produced high and positive r values for R_s (0.928) and for the temperature attributes (0.855 for T_{mean} , 0.806 for T_{min} , 0.878 for T_{max}), and lower and negative r values for the relative humidity (-0.549

for RH_{mean} , -0.578 for RH_{min} and -0.468 for RH_{max} , whereas the effect of wind speed appears to be weaker ($r = +0.226$).

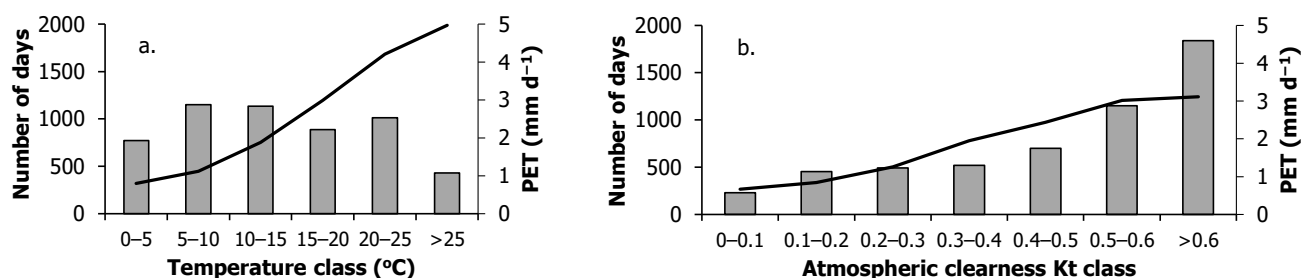


Figure 5. Frequency distributions (bars) and average potential evapotranspiration PET values (lines) for different (a) daily mean air temperatures and (b) atmospheric clearness conditions in Chrysopigi, for the period 2008–2023.

The above patterns suggest that solar radiation is the main attribute determining PET; however, in regions with low meteorological data availability, the estimations of PET by using temperature data might be a meaningful alternative. In conjunction with the estimates of the daily extraterrestrial radiation R_a (which is estimated by only the geographical latitude of each site), PET can be estimated with accuracy, also considering the strong correlation between R_a and PET ($r = +0.863$).

3.2. PET Estimates and Comparisons

The estimation of daily PET by models incorporating only temperature attributes (Equations (1)–(36)) is presented comparatively with the estimates of the FAO56–PM benchmark method in Figure 6. Most PET = $f(T)$ equations presented high R^2 values (higher than 0.85), and two of them, Equation (19), Droogers & Allen 2002 (1), and Equation (26), Trajkovic 2007, presented the best R^2 (0.902).

The inclusion of water-related attributes as relative humidity or precipitation does not affect the accuracy of PET in Chrysopigi (Figure 7). The dispersion of values against the benchmark method indicates the good performance of the tested models. However, the R^2 values are, in general, lower, ranging from 0.682 (Equation (38), Schendel 1967) to 0.885 (Equation (47), Ahooghalaandari et al. 2016 (4)), while none of the models showed R^2 higher than 0.9. It should be stated, however, that six out of the 14 tested PET = $f(T, RH$ or PR) models presented R^2 higher than 0.85.

More statistical indices to perform an accurate evaluation of the performance of the 50 tested models, along with their overall ranking, are presented in Tables 3 and 4. For the group of the PET = $f(T)$ estimates, the average values range from 1.988 mm d^{-1} (Equation (3), McCloud 1955) to 3.676 mm d^{-1} (Equation (17), Xu & Singh 2001 (3)), which correspond to -18.1% and $+51.4\%$ deviations from the FAO56–PM average value (2.428 mm d^{-1}), respectively. It is worth noting that most methods (20 out of the 36) of the general form PET = $f(T)$ produced accurate averages with less than 10% difference from the benchmark method, and two of them, i.e., Equation (4), Hamon 1963, and Equation (31), Heydari & Heydari 2014, had averages with differences less than 1%. In addition, Equation (36), Proutsos et al. 2023, Model 4, had the best slope value (1.000), whereas Equation (35), Proutsos et al. 2023, Model 3, showed the best offset (-0.009). Similarly, Equation (31), Heydari & Heydari 2014, presented the best MBE (-0.004) and Equation (29), Ravazzani et al. 2012, had the best RMSE (0.519), MAE (0.346), and d (0.979).

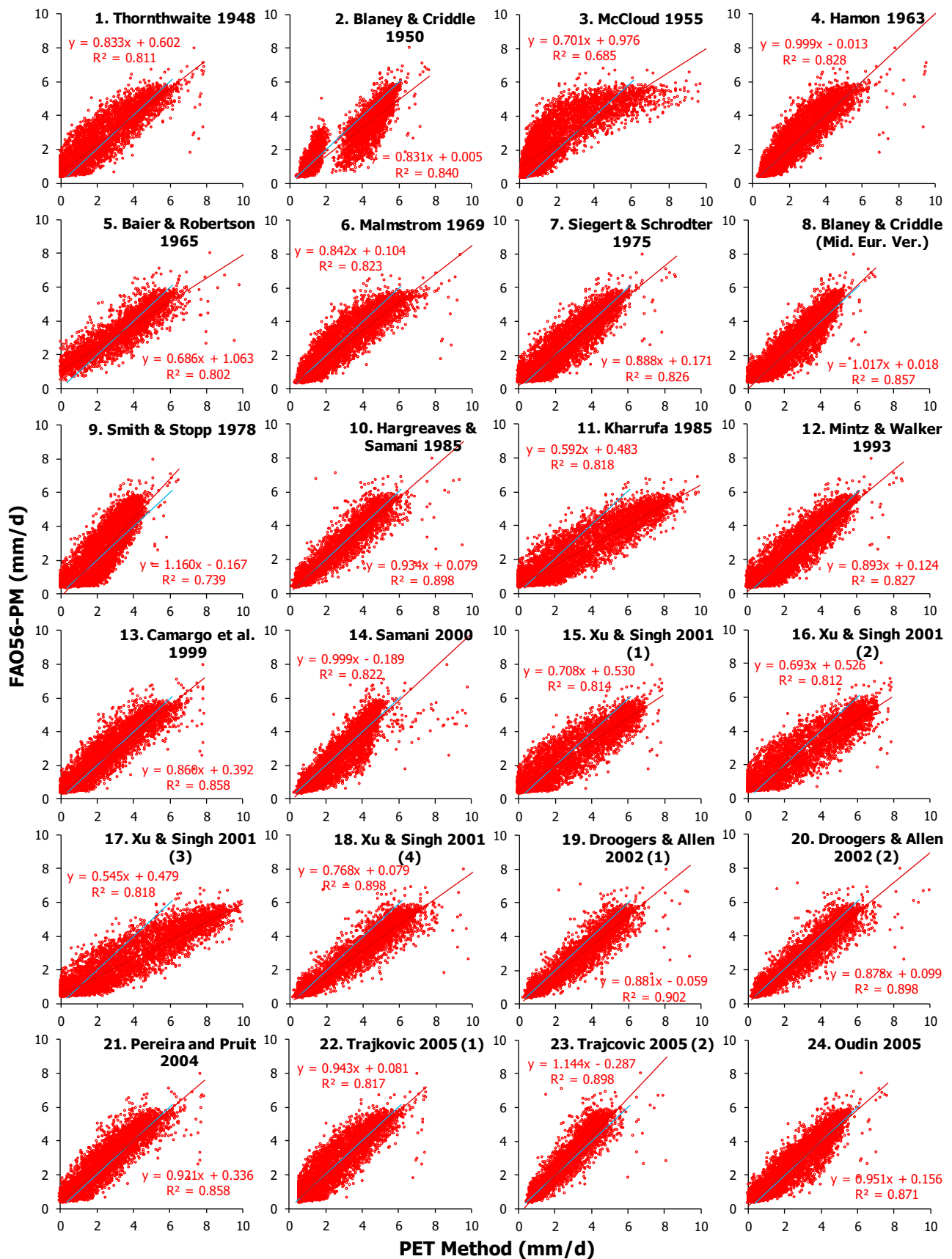


Figure 6. Cont.

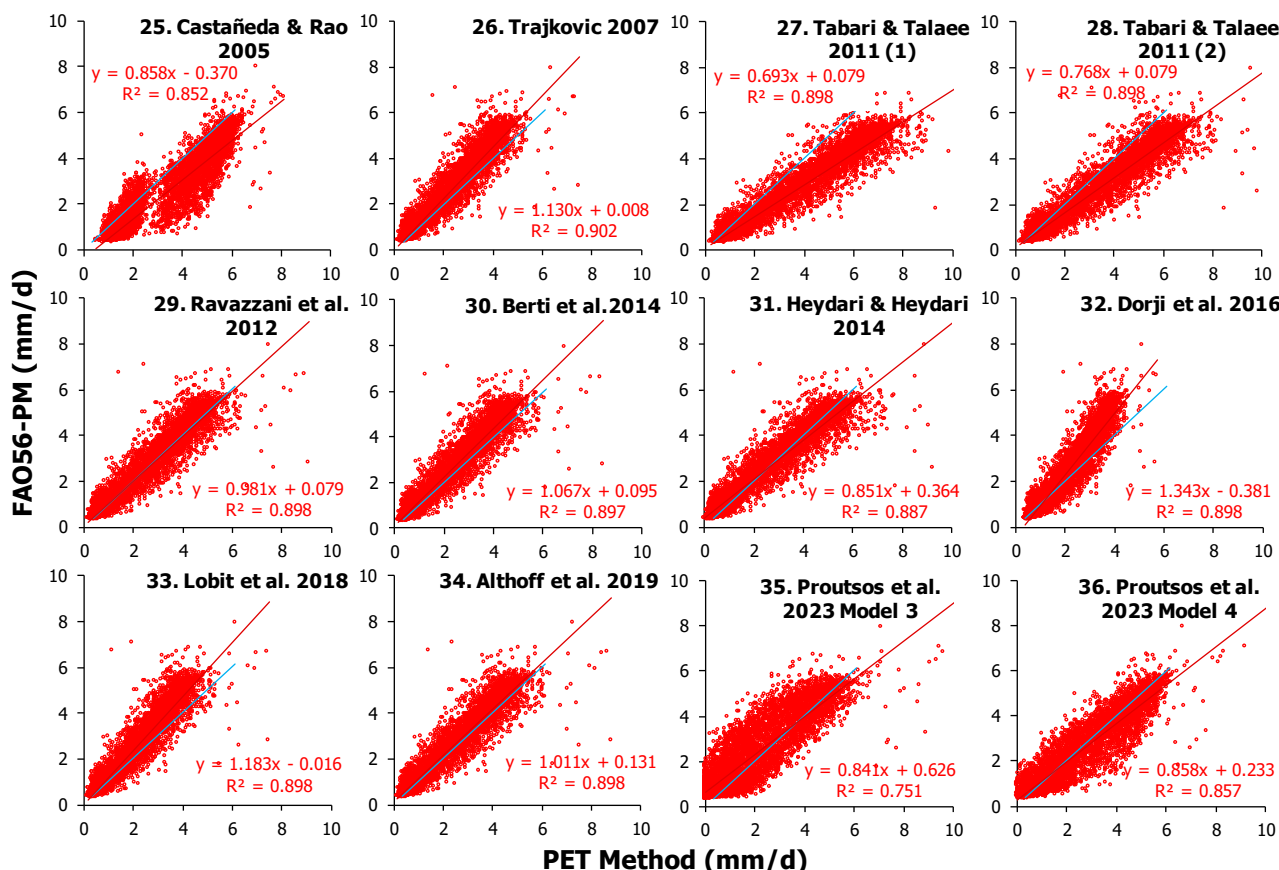


Figure 6. Correlation between daily PET values estimated by different temperature (T)-based methods (x-axis) of the general form $PET = f(T)$ against the benchmark FAO56-PM method (y-axis) for the forest site of Chrysopigi, Greece, along with the linear regression statistics. The blue line indicates the 1:1 regression.

Table 3. Statistical indices (mean, slope a , intercept b , coefficient of determination R^2 , of the linear regression $y = ax + b$; mean bias error MBE; root mean square error RMSE; mean absolute error MAE; standard deviation square sd^2 ; and index of agreement d) for the 36 models of the $PET = f(T)$ group compared to the FAO56-PM benchmark method, at the forest site of Chrysopigi. The ranking (sRPI score and Rank) is based on the optimum values of the indices for all tested 50 PET models.

PET = f(T) Method	N	Mean	a	b	MBE	RMSE	MAE	sd ²	d	R ²	sRPI	Rank
FAO56-PM	5389	2.428										
1. Thornthwaite 1948	4394	2.273	0.973	-0.155	-0.222	0.794	0.604	0.580	0.961	0.811	0.881	19
2. Blaney & Criddle 1950	5615	2.858	1.011	0.462	0.527	0.906	0.691	0.542	0.938	0.840	0.844	26
3. McCloud 1955	5602	1.988	0.977	-0.305	-0.335	1.107	0.785	1.113	0.907	0.685	0.735	37
4. Hamon 1963	5389	2.444	0.829	0.431	0.016	0.672	0.516	0.452	0.960	0.828	0.877	21
5. Baier & Robertson 1965	3529	3.242	1.170	-0.604	-0.044	0.817	0.627	0.665	0.942	0.802	0.823	32
6. Malmstrom 1969	5389	2.761	0.977	0.389	0.333	0.808	0.623	0.542	0.955	0.823	0.863	25
7. Siegert & Schrodter 1975	5218	2.603	0.930	0.293	0.120	0.708	0.556	0.487	0.957	0.826	0.887	18
8. Blaney & Criddle (MEV)	5539	2.320	0.843	0.327	-0.034	0.615	0.484	0.377	0.963	0.857	0.909	15
9. Smith & Stopp 1978	5218	2.284	0.637	0.703	-0.199	0.871	0.713	0.719	0.890	0.739	0.718	38
10. Hargreaves-Samani 1985	5389	2.514	0.961	0.180	0.086	0.535	0.352	0.279	0.964	0.898	0.969	2
11. Kharrufa 1985	5218	3.382	1.382	-0.051	0.898	1.516	1.167	1.493	0.870	0.818	0.691	39
12. Mintz & Walker 1993	5218	2.644	0.927	0.342	0.160	0.713	0.562	0.483	0.972	0.827	0.887	17
13. Camargo et al. 1999	5375	2.374	0.997	-0.053	-0.059	0.661	0.494	0.433	0.962	0.858	0.943	8
14. Samani 2000	5385	2.618	0.823	0.621	0.192	0.710	0.515	0.466	0.950	0.822	0.844	27
15. Xu & Singh 2001 (1)	4394	2.776	1.150	-0.092	0.281	0.964	0.765	0.850	0.925	0.814	0.831	30
16. Xu & Singh 2001 (2)	4394	2.839	1.172	-0.085	0.344	1.012	0.802	0.906	0.943	0.812	0.827	31
17. Xu & Singh 2001 (3)	5216	3.676	1.501	-0.049	1.193	1.840	1.416	1.960	0.867	0.818	0.621	41
18. Xu & Singh 2001 (4)	5389	3.061	1.170	0.219	0.633	0.940	0.703	0.484	0.964	0.898	0.880	20

Table 3. Cont.

PET = f(T) Method	N	Mean	a	b	MBE	RMSE	MAE	sd ²	d	R ²	sRPI	Rank
19. Droog. & Allen 2002 (1)	5389	2.824	1.025	0.336	0.396	0.676	0.496	0.300	0.970	0.902	0.934	11
20. Droog. & Allen 2002 (2)	5389	2.654	1.023	0.169	0.226	0.603	0.402	0.313	0.971	0.898	0.961	4
21. Pereira and Pruit 2004	5375	2.277	0.931	0.011	-0.156	0.644	0.478	0.390	0.963	0.858	0.936	10
22. Trajkovic 2005 (1)	4592	2.479	0.867	0.385	0.064	0.701	0.547	0.488	0.952	0.817	0.869	23
23. Trajkovic 2005 (2)	5615	2.292	0.785	0.467	-0.039	0.547	0.410	0.298	0.968	0.898	0.926	14
24. Oudin 2005	5606	2.319	0.916	0.165	-0.015	0.588	0.436	0.345	0.961	0.871	0.942	9
25. Castañeda & Rao 2005	5615	3.195	0.993	0.850	0.865	1.103	0.919	0.469	0.895	0.852	0.769	36
26. Trajkovic 2007	5389	2.141	0.798	0.204	-0.287	0.610	0.437	0.290	0.963	0.902	0.930	13
27. Tabari & Talaei 2011 (1)	5389	3.389	1.296	0.242	0.960	1.285	1.000	0.730	0.876	0.898	0.772	34
28. Tabari & Talaei 2011 (2)	5389	3.061	1.170	0.219	0.633	0.940	0.703	0.484	0.957	0.898	0.877	22
29. Ravazzani et al. 2012	5389	2.394	0.915	0.171	-0.034	0.519	0.346	0.268	0.979	0.898	0.974	1
30. Berti et al. 2014	5389	2.187	0.841	0.145	-0.241	0.581	0.406	0.279	0.963	0.897	0.943	7
31. Heydari & Heydari 2014	5389	2.424	1.041	-0.104	-0.004	0.607	0.387	0.369	0.965	0.887	0.964	3
32. Dorji et al. 2016	5389	2.091	0.668	0.468	-0.337	0.732	0.536	0.422	0.938	0.898	0.866	24
33. Lobit et al. 2018	5389	2.066	0.759	0.223	-0.363	0.675	0.482	0.325	0.929	0.898	0.898	16
34. Althoff et al. 2019	5389	2.273	0.888	0.116	-0.156	0.541	0.370	0.268	0.964	0.898	0.960	5
35. Proutsos et al. 2023 M3	5218	2.208	0.893	-0.009	-0.276	0.893	0.691	0.721	0.932	0.751	0.820	33
36. Proutsos et al. 2023 M4	5353	2.573	1.000	0.134	0.133	0.674	0.489	0.436	0.961	0.857	0.932	12

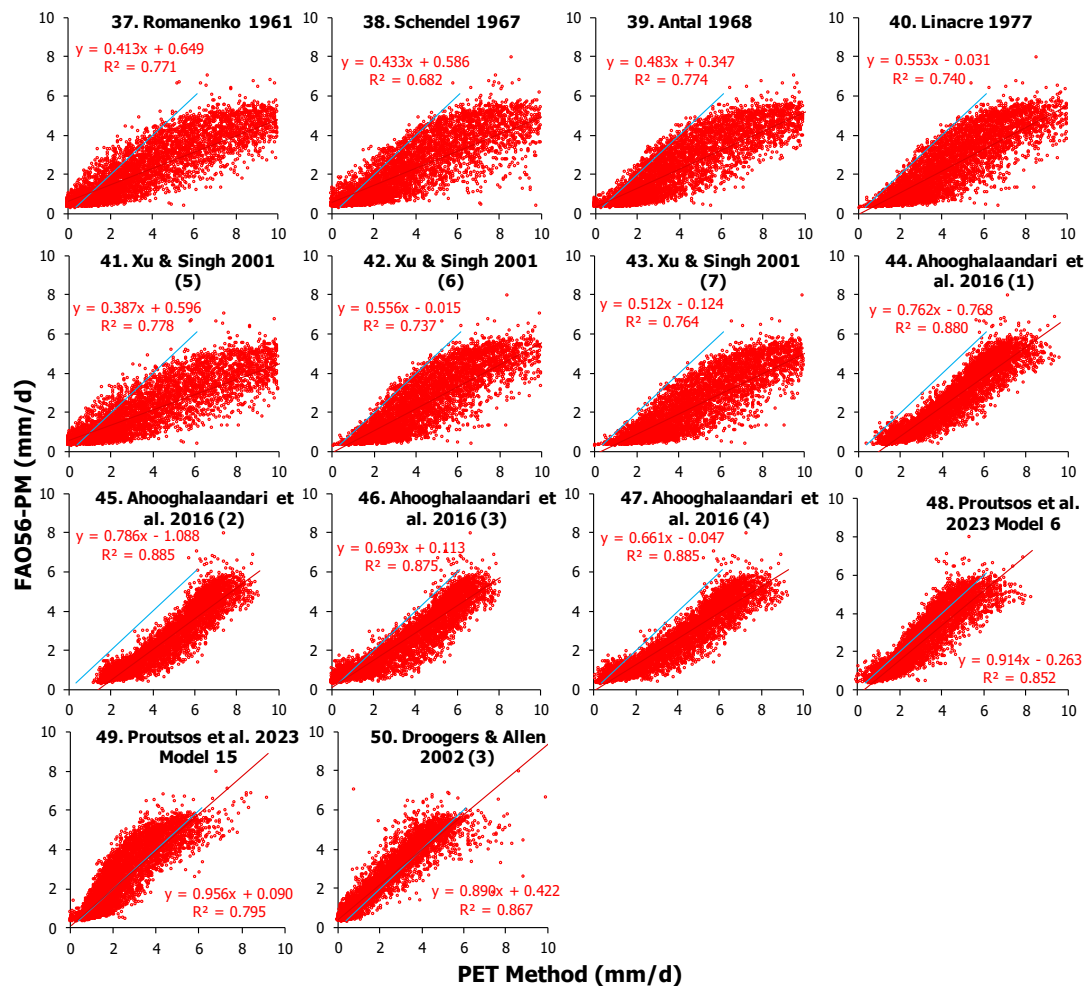


Figure 7. Correlation between daily PET values estimated by different temperature-based methods (x-axis) corrected with relative humidity (RH) or precipitation (PR) attributes, following the general forms $PET = f(T, RH)$ (Equations (37)–(49)) and $PET = f(T, PR)$ (Equation (50)) against the benchmark FAO56-PM method (y-axis) for the forest sites of Chrysopigi, Greece, along with the linear regression statistics. The blue line indicates the 1:1 regression.

Table 4. Statistical indices (mean, slope a , intercept b , and coefficient of determination R^2 , of the linear regression $y = ax + b$; mean bias error MBE; root mean square error RMSE; mean absolute error MAE; standard deviation square sd^2 ; and index of agreement d) for the 36 models of the PET = f (RH or PR) groups compared to the FAO56-PM benchmark method, at the forest site of Chrysopigi. The ranking (sRPI score and Rank) is based on the optimum values of the indices for all tested 50 PET models.

PET = f (RH or PR) Method	N	Mean	a	b	MBE	RMSE	MAE	sd^2	d	R^2	sRPI	Rank
37. Romanenko 1961	5578	4.239	1.865	−0.233	1.925	2.879	2.047	4.580	0.676	0.771	0.275	49
38. Schendel 1967	5083	4.240	1.575	0.425	1.817	2.656	1.895	3.753	0.799	0.682	0.342	47
39. Antal 1968	5376	4.303	1.604	0.416	1.880	2.540	1.906	2.918	0.861	0.774	0.438	44
40. Linacre 1977	5383	4.442	1.339	1.194	2.017	2.453	2.021	1.951	0.865	0.740	0.412	46
41. Xu & Singh 2001 (5)	5516	4.586	2.008	−0.172	2.302	3.278	2.397	5.446	0.738	0.778	0.214	50
42. Xu & Singh 2001 (6)	5385	4.389	1.325	1.174	1.962	2.402	1.967	1.922	0.890	0.737	0.432	45
43. Xu & Singh 2001 (7)	5374	4.975	1.492	1.362	2.553	2.993	2.554	2.438	0.811	0.764	0.279	48
44. Ahooghal. et al., 2016 (1)	5615	4.141	1.156	1.390	1.810	1.967	1.812	0.591	0.901	0.880	0.591	42
45. Ahooghal. et al., 2016 (2)	5615	4.423	1.125	1.741	2.093	2.220	2.094	0.550	0.830	0.885	0.503	43
46. Ahooghal. et al., 2016 (3)	5581	3.312	1.263	0.277	0.969	1.347	1.062	0.873	0.928	0.875	0.771	35
47. Ahooghal. et al., 2016 (4)	5612	3.683	1.339	0.493	1.352	1.671	1.376	0.963	0.886	0.885	0.681	40
48. Proutsos et al., 2023 M. 6	5614	2.887	0.933	0.680	0.557	0.865	0.683	0.438	0.948	0.852	0.836	29
49. Proutsos et al., 2023 M. 15	5387	2.446	0.832	0.426	0.017	0.736	0.576	0.542	0.938	0.795	0.841	28
50. Droog. & Allen 2002 (3)	5357	2.264	0.974	−0.109	−0.174	0.643	0.421	0.383	0.976	0.867	0.947	6

The statistics for the PET = f (RH or PR) group are overall worse than the PET = f(T) group, as shown in Tables 3 and 4. However, Equation (49), Proutsos et al. 2023, Model 15, and Equation (50), Droogers & Allen 2002 (3), produced PET averages that were less than 10% different from the benchmark method (+0.7 and +6.8%, respectively). In this category, Equation (47), Ahooghalaandari et al. 2016 (4), presented the best R^2 (0.885), and Equation (49), Proutsos et al. 2023, Model 15, the best MBE (0.017), but Equation (50), Droogers & Allen 2002 (3), showed the best statistics in the slope (0.974) and the offset (−0.109) of the linear regression, the RMSE (0.643), MAE (0.421), sd^2 (0.383), and d (0.976).

3.3. PET Methods Ranking

The overall assessment of all indices and the ranking of all the tested models for the forest site of Chrysopigi is presented in Table 3 and in Figure 8. Twelve out of the 50 tested methods showed sRPI scores higher than 0.90 and four of them reached scores higher than 0.95 as follows: Equation (29), Ravazzani et al. 2012; Equation (10), Hargreaves & Samani 1985; Equation (31) Heydari & Heydari 2014; Equation (20) Droogers & Allen 2002 (2); and Equation (34) Althoff et al., 2019. On the contrary, Equation (39), Antal 1968; Equation (42), Xu & Singh 2001 (6); Equation (40), Linacre 1977; Equation (38), Schendel 1967; Equation (43), Xu & Singh 2001 (7); Equation (37), Romanenko 1961; and Equation (41), Xu & Singh 2001 (5) performed worse at the studied forest site and presented very low sRPI scores (less than 0.500).

The best performing method (Equation (29), Ravazzani et al. 2012) showed an average PET of 2.349 mm d^{-1} and was only by −1.4% different compared to the benchmark method. Worth noting is the performance of the widely used Equation (10), Hargreaves and Samani, method, which is ranked 2nd among all the 50 models, with an average PET (2.514 mm d^{-1}) that was 3.5% higher than the benchmark.

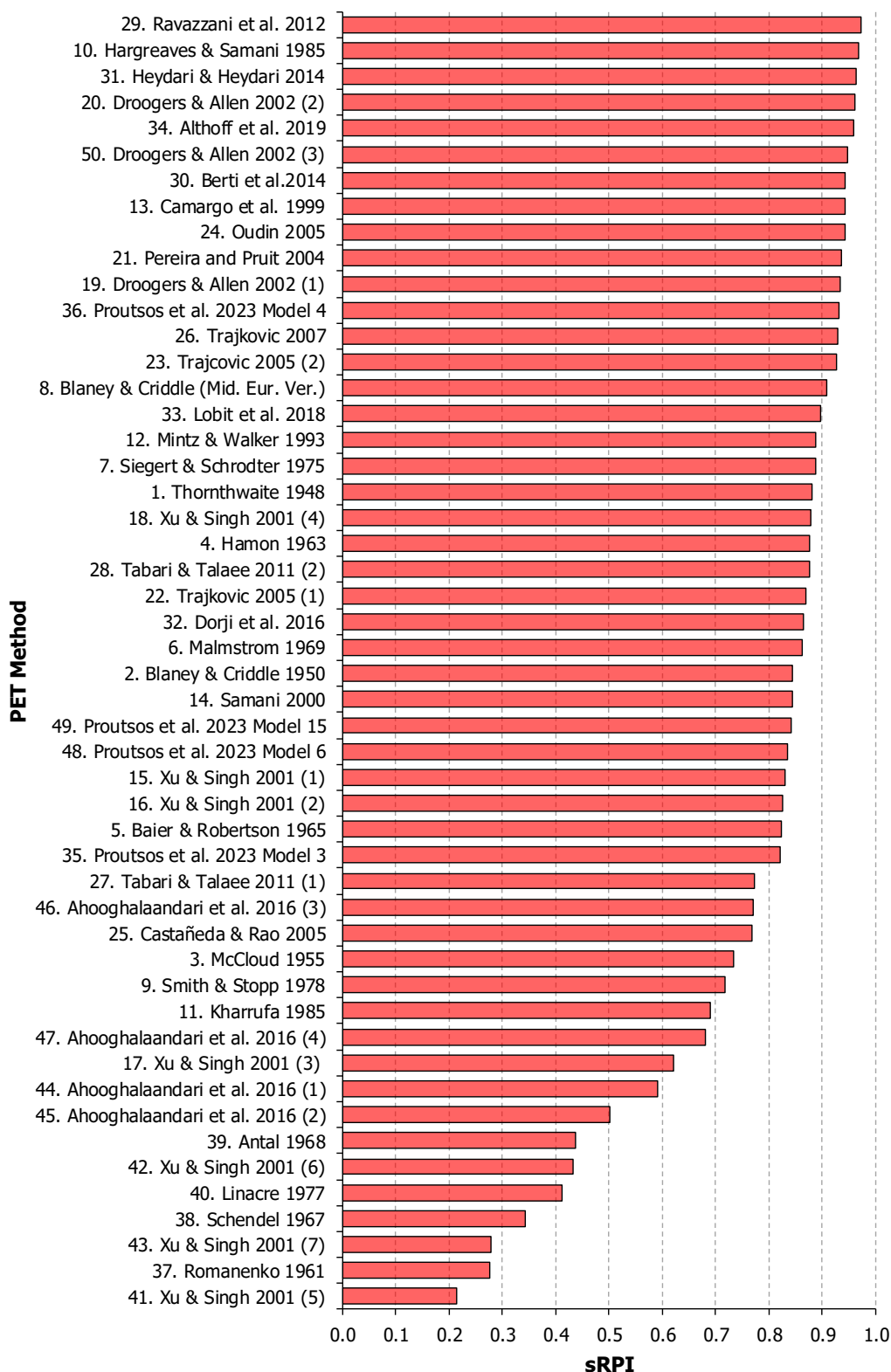


Figure 8. Rank scores based on the sRPI index and ranking of the 50 temperature-based PET methods at the forest site of Chrysopigi, Greece.

4. Discussion

The superior performance of radiation-based methods compared to temperature-based ones for the estimation of PET is widely acknowledged [88]. However, temperature-based

models also exhibit adequate behavior and are preferred in many studies due to their lower data requirements and the greater availability of temperature data compared to radiation.

In our forest site, various temperature-based methods demonstrated differing performance. The calculated PET average values ranged from 1.988 mm/d to 4.975 mm/d, resulting in differences with the FAO–56 PM benchmark method (2.428 mm–d). These differences suggest either underestimation or overestimation of PET values by percentages ranging from -18% to $+105\%$. Specifically, 33 out of the 50 tested methods overestimated PET, while the remaining 17 underestimated it. However, 22 methods produced average PET values with less than a 10% difference from the benchmark method's average. The five best-performing methods exhibited PET averages that differed from -6% (Equation (34), Althoff et al. 2019) to $+9\%$ (Equation (20), Droogers & Allen 2002 (2)) from the benchmark method's mean PET, while Equation (31), Heydari & Heydari 2014, showed the smallest difference (-0.2%).

The equation proposed by Ravazzani et al. 2012 demonstrates an overall superior performance compared to all other temperature-based models, followed by the original Equation (31), Hargreaves–Samani model 1985; Equation (20), Heydari & Heydari 2014; Equation (20), Droogers & Allen 2002 (2); and Equation (34), Althoff et al. 2019 methods, all of which exhibited high rank scores ($sRPI > 0.95$). Ravazzani et al. (2012) along with all the aforementioned models are actually modifications of the Hargreaves–Samani 1985 model. Notably, Ravazzani et al. 2012 incorporated an altitude-related term into the original Hargreaves–Samani equation. The commendable performance of the original Hargreaves–Samani model aligns with the findings of Lang et al. (2017), who investigated the performance of eight PET methods in southwest China and recommended this specific method as the best temperature-based method for the area. It should be highlighted that the aforementioned five best-performing methods are solely temperature-related, classified into the $PET = f(T)$ group, without incorporating any water-related (RH or precipitation) factors. This suggests that an increase in the number of input parameters does not necessarily lead to more accurate PET estimates, at least not in the specific Mediterranean forest environment.

Among the group of models incorporating temperature and relative humidity, or precipitation ($PET = f(T, RH \text{ or } PR)$), Proutsos et al. 2023, Model 15 and Model 6, along with the equations by Ahooghalaandari et al. 2016 (3), (4), and (1), produced the most accurate PET estimates, exhibiting relatively higher rank scores compared to other equations in this category. However, PET estimates from this group of methods differed, on average, by $+60\%$, ranging from -7% (Droogers and Allen 2002 (3)) to $+105\%$ (Xu and Singh 2001 (7)). Notably, the models by Droogers and Allen 2002 (3) and Proutsos et al. 2023, Model 15, emerged as the top performers in this category, ranking 6th and 28th among all examined methods, with average PET differences of -7% and $+0.7\%$, respectively.

The method proposed by Ravazzani et al. 2012 was identified as the overall best-performing method, with an average PET of 2.394, being only by -1.4% different from the benchmark method. However, this method exhibited poorer performance when applied in urban green areas. In the study of Proutsos et al. [23], Ravazzani et al. 2012 ranked 32nd among 52 examined temperature-based methods, indicating that urban environments or variations in latitude and altitude may affect its accuracy. Similar discrepancies were observed for other top-performing methods at the forest site of Chrysopigi, such as the original Hargreaves–Samani 1985 model, which ranked 2nd in this study but 25th among 52 methods in urban sites. Similarly, Heydari & Heydari 2014, Droogers & Allen 2002 (2), and Althoff et al. 2019, ranked 3rd, 4th, and 5th, respectively, in this study, but were 21st, 31st, and 26th among temperature-based methods in urban sites.

Previous studies suggest that the best-performing temperature-based methods in urban sites differ from those in forest environments. For example, Ahooghalaandari et al. 2016 (3), Oudin 2005, and Xu & Singh 2001 (2) and (1) were ranked 12th, 35th, 9th, 31st, and 30th, respectively, when applied to the studied forest site. In the forest site studied by Bourletsikas et al. [46] in central Greece, almost all temperature-based models showed good performance with slight underestimation of PET. The original Hargreaves–Samani

method and its modifications performed well, consistent with the findings of Valipour and Eslamian [34] and Valipour [89] at various Iranian provinces. Our results are also in line with the findings of Tabari et al. [27] and Trajkovic and Kolakovic [90], using, though, monthly data, who also found that the equation of Hargreaves–Samani and its modifications overestimate PET under humid conditions, but identified poor performance of the Thornthwaite model. A systematic overestimation of Hargreaves–Samani, was also addressed by Alexandris et al. [91], who estimated PET by five empirical models, above rainfed grass in central Serbia and compared the results against the FAO–56 PM benchmark method.

Gebhart et al. [45] evaluated the performance of 13 PET models in Greek forest sites and confirmed an overall better performance of the radiation-based methods against the temperature-based ones, attributing it to the large influence of solar radiation on the determination of the PET fluxes. Regarding the temperature-based models the authors suggested Hammon, McGuinness, and Hargreaves as best performing with regard to their latitudinal distribution. Forest type may also influence evapotranspiration fluxes. Rao et al. [43] compared the monthly measured actual evapotranspiration in two small forested watersheds (conifer plantation and naturally regenerated deciduous hardwoods) in the humid Appalachians in the southeastern U.S. with the PET estimates from three empirical methods (FAO–56 PM, Priestley–Taylor, and Hamon) and found that the annual PET of conifers was higher than of deciduous hardwoods and that Hamon’s and the FAO–56 PM equations generally underestimate the forest PET.

5. Conclusions

In the present study, 50 temperature-based methods for estimating potential evapotranspiration (PET) were compared against the widely used FAO–56 PM benchmark method, known for producing accurate PET estimates. Daily meteorological data from a forest sub-humid site in Chrysopigi (northern Greece) spanning 16 years (2008–2023) were utilized. The resulting PET estimates were evaluated using several statistical indices and were ranked accordingly.

The findings suggest that temperature-based methods can serve as suitable alternatives for PET estimation in forest environments. The performance of the original Hargreaves–Samani model and its modifications was quite efficient for estimating PET in the Mediterranean forest environment. The average daily PET at the studied forest was 2.428 mm, while the tested models produced averages ranging from 1.988 mm/d to 4.975 mm/d, indicating potential overestimation of PET by up to +105% or underestimation by –18%. Among the tested models, 33 overestimated PET and 17 underestimated PET, with 22 showing deviations of less than 10% from the average PET estimated by the benchmark method.

Temperature-based models relying solely on temperature appear to be more suitable for use in Mediterranean forest environments compared to methods incorporating water-related parameters, such as relative humidity or precipitation. The equations of Ravazzani et al., proposed in 2012, followed by Hargreaves–Samani in 1985, Heydari & Heydari in 2014, Droogers & Allen in 2002, model 2, and Althoff et al. in 2019, emerged as the top five performing methods with rank (sRPI index) scores exceeding 0.95, recommending their application in Mediterranean forest areas with limited data. However, further research is necessary at various sites to evaluate the models’ performance. Future work should include assessing the performance of radiation-based and combination methods for PET estimation in natural and urban forests and other green areas, as well as testing temperature and mass-transfer PET methods in different forest areas in Greece.

Author Contributions: Conceptualization, N.D.P.; data curation, N.D.P. and M.N.F.; formal analysis, N.D.P., M.N.F., S.P.S. and D.T.; funding acquisition, N.D.P. and M.N.F.; investigation, N.D.P., M.N.F., S.P.S. and D.T.; methodology, N.D.P., M.N.F., S.P.S. and D.T.; resources, N.D.P., M.N.F., S.P.S. and D.T.; supervision, N.D.P.; validation, N.D.P., M.N.F. and D.T.; visualization, S.P.S. and D.T.; writing—original draft, N.D.P. and S.P.S.; writing—review and editing, N.D.P., M.N.F., S.P.S. and D.T. All authors have read and agreed to the published version of the manuscript.

Funding: This research was supported by the research project “Meteo–FRI” of the Forest Research Institute, as well as by the project “Bioclima and natural vegetation in Greece” of the Institute of Mediterranean Forest Ecosystems, both funded by the Hellenic Agricultural Organization—DIMITRA, for maintaining the operation of Chrysopigi’s meteorological station and for conducting this research.

Institutional Review Board Statement: Not applicable.

Informed Consent Statement: Not applicable.

Data Availability Statement: The data presented in this study are available on request from the corresponding author due to privacy.

Acknowledgments: We acknowledge John Mamanis and Spyros Patropoulos from Scientact S.A. for their support in data acquisition from the studied meteorological station. We would also like to thank Kalliopi Radoglou and George Halivopoulos for the maintenance of the station during part of the study period. The authors highly acknowledge the meaningful comments and suggestions of the four anonymous reviewers that enhanced the quality of the present study.

Conflicts of Interest: The authors declare no conflicts of interest.

References

1. Fotelli, M.N.; Korakaki, E.; Paparrizos, S.A.; Radoglou, K.; Awada, T.; Matzarakis, A. Environmental controls on the seasonal variation in gas exchange and water balance in a near-coastal Mediterranean *Pinus halepensis* forest. *Forests* **2019**, *10*, 313. [[CrossRef](#)]
2. Fotelli, M.N.; Nahm, M.; Radoglou, K.; Rennenberg, H.; Halyvopoulos, G.; Matzarakis, A. Seasonal and interannual ecophysiological responses of beech (*Fagus sylvatica*) at its south-eastern distribution limit in Europe. *For. Ecol. Manag.* **2009**, *257*, 1157–1164. [[CrossRef](#)]
3. Jayathilake, D.I.; Smith, T. Understanding the role of hydrologic model structures on evapotranspiration-driven sensitivity. *Hydrol. Sci. J.* **2020**, *65*, 1474–1489. [[CrossRef](#)]
4. Jia, W.; Zhang, Y.; Wei, Z.; Zheng, Z.; Xie, P. Daily reference evapotranspiration prediction for irrigation scheduling decisions based on the hybrid PSO-LSTM model. *PLoS ONE* **2023**, *18*, e0281478. [[CrossRef](#)] [[PubMed](#)]
5. Nedkov, S.; Campagne, S.; Borisova, B.; Krpec, P.; Prodanova, H.; Kokkoris, I.P.; Hristova, D.; Le Clec’h, S.; Santos-Martin, F.; Burkhard, B. Modeling water regulation ecosystem services: A review in the context of ecosystem accounting. *Ecosyst. Serv.* **2022**, *56*, 101458. [[CrossRef](#)]
6. Proutsos, N.D.; Tsiros, I.X.; Nastos, P.; Tsaousidis, A. A note on some uncertainties associated with Thornthwaite’s aridity index introduced by using different potential evapotranspiration methods. *Atmos. Res.* **2021**, *260*, 105727. [[CrossRef](#)]
7. Roy, D.K. Long short-term memory networks to predict one-step ahead reference evapotranspiration in a subtropical climatic zone. *Environ. Process.* **2021**, *8*, 911–941. [[CrossRef](#)]
8. Stefanidis, S.; Rossiou, D.; Proutsos, N. Drought Severity and Trends in a Mediterranean Oak Forest. *Hydrology* **2023**, *10*, 167. [[CrossRef](#)]
9. Tsiros, I.X.; Nastos, P.; Proutsos, N.D.; Tsaousidis, A. Variability of the aridity index and related drought parameters in Greece using climatological data over the last century (1900–1997). *Atmos. Res.* **2020**, *240*, 104914. [[CrossRef](#)]
10. Boast, C.; Robertson, T. A “micro-lysimeter” method for determining evaporation from bare soil: Description and laboratory evaluation. *Soil. Sci. Soc. Am. J.* **1982**, *46*, 689–696. [[CrossRef](#)]
11. Jia, X.; Dukes, M.D.; Jacobs, J.M.; Irmak, S. Weighing lysimeters for evapotranspiration research in a humid environment. *Trans. ASABE* **2006**, *49*, 401–412. [[CrossRef](#)]
12. Hirschi, M.; Michel, D.; Lehner, I.; Seneviratne, S.I. A site-level comparison of lysimeter and eddy covariance flux measurements of evapotranspiration. *Hydrol. Earth Syst. Sci.* **2017**, *21*, 1809–1825. [[CrossRef](#)]
13. Liu, S.; Xu, Z.; Zhu, Z.; Jia, Z.; Zhu, M. Measurements of evapotranspiration from eddy-covariance systems and large aperture scintillometers in the Hai River Basin, China. *J. Hydrol.* **2013**, *487*, 24–38. [[CrossRef](#)]
14. Xiang, K.; Li, Y.; Horton, R.; Feng, H. Similarity and difference of potential evapotranspiration and reference crop evapotranspiration—a review. *Agric. Water Manag.* **2020**, *232*, 106043. [[CrossRef](#)]
15. Alexandris, S.; Proutsos, N. How significant is the effect of the surface characteristics on the Reference Evapotranspiration estimates? *Agric. Water Manag.* **2020**, *237*, 106181. [[CrossRef](#)]
16. Doorenbos, J.; Pruitt, W. Crop water requirements. In *FAO Irrigation and Drainage Paper 24*; Land and Water Development Division; FAO: Rome, Italy, 1977; p. 144.
17. Penman, H.L. Natural evaporation from open water, bare soil and grass. *Proc. R. Soc. London. Ser. A. Math. Phys. Sci.* **1948**, *193*, 120–145. [[CrossRef](#)]
18. Proutsos, N.; Tigkas, D.; Tsevreni, I.; Tsevreni, M. Drought Assessment in Nestos River Basin (N. Greece) for the Period 1955–2018. In *Proceedings of the 10th International Conference on Information and Communication Technologies in Agriculture, Food and Environment, HAICTA 2022, Athens, Greece, 22–25 September 2022*; pp. 429–437.

19. Tegos, A.; Stefanidis, S.; Cody, J.; Koutsoyiannis, D. On the Sensitivity of Standardized-Precipitation-Evapotranspiration and Aridity Indexes Using Alternative Potential Evapotranspiration Models. *Hydrology* **2023**, *10*, 64. [[CrossRef](#)]
20. Vangelis, H.; Tigkas, D.; Tsakiris, G. The effect of PET method on Reconnaissance Drought Index (RDI) calculation. *J. Arid. Environ.* **2013**, *88*, 130–140. [[CrossRef](#)]
21. Allen, R.G.; Pereira, L.S.; Raes, D.; Smith, M. *Crop Evapotranspiration-Guidelines for Computing Crop Water Requirements-FAO Irrigation and Drainage Paper 56*; FAO: Rome, Italy, 1998; Volume 300, p. D05109.
22. Allen, R.G.; Clemmens, A.J.; Burt, C.M.; Solomon, K.; O'Halloran, T. Prediction accuracy for projectwide evapotranspiration using crop coefficients and reference evapotranspiration. *J. Irrig. Drain. Eng.* **2005**, *131*, 24–36. [[CrossRef](#)]
23. Proutsos, N.; Tigkas, D.; Tsevereni, I.; Alexandris, S.G.; Solomou, A.D.; Bourletsikas, A.; Stefanidis, S.; Nwokolo, S.C. A Thorough Evaluation of 127 Potential Evapotranspiration Models in Two Mediterranean Urban Green Sites. *Remote Sens.* **2023**, *15*, 3680. [[CrossRef](#)]
24. Xu, L.; Shi, Z.; Wang, Y.; Zhang, S.; Chu, X.; Yu, P.; Xiong, W.; Zuo, H.; Wang, Y. Spatiotemporal variation and driving forces of reference evapotranspiration in Jing River Basin, northwest China. *Hydrol. Process.* **2015**, *29*, 4846–4862. [[CrossRef](#)]
25. Trajkovic, S. Comparison of radial basis function networks and empirical equations for converting from pan evaporation to reference evapotranspiration. *Hydrol. Process. Int. J.* **2009**, *23*, 874–880. [[CrossRef](#)]
26. Droogers, P.; Allen, R.G. Estimating reference evapotranspiration under inaccurate data conditions. *Irrig. Drain. Syst.* **2002**, *16*, 33–45. [[CrossRef](#)]
27. Tabari, H.; Talaee, P.H. Local calibration of the Hargreaves and Priestley-Taylor equations for estimating reference evapotranspiration in arid and cold climates of Iran based on the Penman-Monteith model. *J. Hydrol. Eng.* **2011**, *16*, 837–845. [[CrossRef](#)]
28. Islam, S.; Alam, A.R. Performance evaluation of FAO Penman-Monteith and best alternative models for estimating reference evapotranspiration in Bangladesh. *Heliyon* **2021**, *7*, e07487. [[CrossRef](#)]
29. Kisi, O. Comparison of different empirical methods for estimating daily reference evapotranspiration in Mediterranean climate. *J. Irrig. Drain. Eng.* **2014**, *140*, 04013002. [[CrossRef](#)]
30. Li, S.; Kang, S.; Zhang, L.; Zhang, J.; Du, T.; Tong, L.; Ding, R. Evaluation of six potential evapotranspiration models for estimating crop potential and actual evapotranspiration in arid regions. *J. Hydrol.* **2016**, *543*, 450–461. [[CrossRef](#)]
31. Paparrizos, S.; Maris, F.; Matzarakis, A. Sensitivity analysis and comparison of various potential evapotranspiration formulae for selected Greek areas with different climate conditions. *Theor. Appl. Climatol.* **2017**, *128*, 745–759. [[CrossRef](#)]
32. Samaras, D.A.; Reif, A.; Theodoropoulos, K. Evaluation of radiation-based reference evapotranspiration models under different Mediterranean climates in central Greece. *Water Resour. Manag.* **2014**, *28*, 207–225. [[CrossRef](#)]
33. Sharafi, S.; Mohammadi Ghaleni, M. Calibration of empirical equations for estimating reference evapotranspiration in different climates of Iran. *Theor. Appl. Climatol.* **2021**, *145*, 925–939. [[CrossRef](#)]
34. Valipour, M.; Eslamian, S. Analysis of potential evapotranspiration using 11 modified temperature-based models. *Int. J. Hydrol. Sci. Technol.* **2014**, *4*, 192–207. [[CrossRef](#)]
35. Xystrakis, F.; Matzarakis, A. Evaluation of 13 empirical reference potential evapotranspiration equations on the island of Crete in southern Greece. *J. Irrig. Drain. Eng.* **2011**, *137*, 211–222. [[CrossRef](#)]
36. Chen, X.; Liu, X.; Zhou, G.; Han, L.; Liu, W.; Liao, J. 50-year evapotranspiration declining and potential causations in subtropical Guangdong province, southern China. *Catena* **2015**, *128*, 185–194. [[CrossRef](#)]
37. Stefanidis, S.; Alexandridis, V. Precipitation and potential evapotranspiration temporal variability and their relationship in two forest ecosystems in Greece. *Hydrology* **2021**, *8*, 160. [[CrossRef](#)]
38. Yassen, A.; Nam, W.; Hong, E. Impact of climate change on reference evapotranspiration in Egypt. *Catena* **2020**, *194*, 104711. [[CrossRef](#)]
39. Proutsos, N.; Tigkas, D. Growth response of endemic black pine trees to meteorological variations and drought episodes in a Mediterranean region. *Atmosphere* **2020**, *11*, 554. [[CrossRef](#)]
40. Sun, G.; Wei, X.; Hao, L.; Sanchis, M.G.; Hou, Y.; Yousefpour, R.; Tang, R.; Zhang, Z. Forest hydrology modeling tools for watershed management: A review. *For. Ecol. Manag.* **2023**, *530*, 120755. [[CrossRef](#)]
41. Federer, C.; Vörösmarty, C.; Fekete, B. Intercomparison of methods for calculating potential evaporation in regional and global water balance models. *Water Resour. Res.* **1996**, *32*, 2315–2321. [[CrossRef](#)]
42. Fisher, J.B.; DeBiase, T.A.; Qi, Y.; Xu, M.; Goldstein, A.H. Evapotranspiration models compared on a Sierra Nevada forest ecosystem. *Environ. Model. Softw.* **2005**, *20*, 783–796. [[CrossRef](#)]
43. Rao, L.; Sun, G.; Ford, C.; Vose, J. Modeling potential evapotranspiration of two forested watersheds in the southern Appalachians. *Trans. ASABE* **2011**, *54*, 2067–2078. [[CrossRef](#)]
44. Ha, W.; Kolb, T.E.; Springer, A.E.; Dore, S.; O'Donnell, F.C.; Martinez Morales, R.; Masek Lopez, S.; Koch, G.W. Evapotranspiration comparisons between eddy covariance measurements and meteorological and remote-sensing-based models in disturbed ponderosa pine forests. *Ecophysiology* **2015**, *8*, 1335–1350. [[CrossRef](#)]
45. Gebhart, S.; Radoglou, K.; Chalivopoulos, G.; Matzarakis, A. Evaluation of potential evapotranspiration in central Macedonia by EmPEst. In *Advances in Meteorology, Climatology and Atmospheric Physics*; Springer: Berlin/Heidelberg, Germany, 2013; pp. 451–456.
46. Bourletsikas, A.; Argyrokastritis, I.; Proutsos, N. Comparative evaluation of 24 reference evapotranspiration equations applied on an evergreen-broadleaved forest. *Hydrol. Res.* **2018**, *49*, 1028–1041. [[CrossRef](#)]

47. Emberger, L. Un projet d'une classification des climats du point de vue phytogéographique. *Bul. Soc. D' Hist. Nat. Toulouse* **1942**, *77*, 97–124.
48. Bagnouls, F.; Gaussen, H. Les climats biologiques et leur classification. *Ann. Géographie* **1957**, *355*, 193–220. [[CrossRef](#)]
49. Mantratzis, P. *The Influence of Canopy Architecture on Kermes oak (Quercus coccifera L.) Ecophysiology*; Aristotle University of Thessaloniki: Thessaloniki, Greece, 2003. (In Greek)
50. Pereira, A.R.; Pruitt, W.O. Adaptation of the Thornthwaite scheme for estimating daily reference evapotranspiration. *Agric. Water Manag.* **2004**, *66*, 251–257. [[CrossRef](#)]
51. Thornthwaite, C.W. An approach toward a rational classification of climate. *Geogr. Rev.* **1948**, *38*, 55–94. [[CrossRef](#)]
52. Blaney, H.; Criddle, W. *Determining Water Requirements in Irrigated Area from Climatological Irrigation Data*; USDA, Soil Conservation Service: Washington, DC, USA, 1950; p. 48.
53. McCloud, D. Water requirements of field crops in Florida as influenced by climate. *Proc. Soil. Sci. Soc. Fla.* **1955**, *15*, 165–172.
54. Dingman, S. *Physical Hydrology*, 2nd ed.; Waveland Pr Inc.: Salem, WI, USA, 2008; p. 656.
55. Hamon, W.R. Computation of direct runoff amounts from storm rainfall. *Int. Assoc. Sci. Hydrol. Publ.* **1963**, *63*, 52–62.
56. Baier, W.; Robertson, G.W. Estimation of latent evaporation from simple weather observations. *Can. J. Plant Sci.* **1965**, *45*, 276–284. [[CrossRef](#)]
57. Siegert, E.; Schrödter, H. Erfahrungen mit dem Wasserbilanzschreiber nach Klausung. *Dtsch. Gewässerkd. Mitteilungen* **1975**, *19*, 167–171.
58. Smith, D.I.; Stopp, P. *The River Basin: An Introduction to the Study of Hydrology*; Cambridge University Press: Cambridge, UK, 1978.
59. Hargreaves, G.H.; Samani, Z.A. Reference crop evapotranspiration from temperature. *Appl. Eng. Agric.* **1985**, *1*, 96–99. [[CrossRef](#)]
60. Kharrufa, N. Simplified equation for evapotranspiration in arid regions. *Beiträge Zur. Hydrol.* **1985**, *5*, 39–47.
61. Mintz, Y.; Walker, G. Global fields of soil moisture and land surface evapotranspiration derived from observed precipitation and surface air temperature. *J. Appl. Meteorol. Climatol.* **1993**, *32*, 1305–1334. [[CrossRef](#)]
62. Camargo, Â.P.d.; Marin, F.R.; Sentelhas, P.C.; Picini, A.G. Ajuste da equação de Thornthwaite para estimar evapotranspiração potencial em climas áridos e superúmidos, com base na amplitude térmica diária. *Rev. Bras. Agrometeorol.* **1999**, *7*, 251–257.
63. Hargreaves, G.; Samani, Z. Estimating potential evapotranspiration. *J. Irrig. Drain. Engr. ASCE* **1982**, *108*, 223–230. [[CrossRef](#)]
64. Samani, Z. Estimating solar radiation and evapotranspiration using minimum climatological data. *J. Irrig. Drain. Eng.* **2000**, *126*, 265–267. [[CrossRef](#)]
65. Xu, C.Y.; Singh, V. Evaluation and generalization of temperature-based methods for calculating evaporation. *Hydrol. Process.* **2001**, *15*, 305–319. [[CrossRef](#)]
66. Trajkovic, S. Temperature-based approaches for estimating reference evapotranspiration. *J. Irrig. Drain. Eng.* **2005**, *131*, 316–323. [[CrossRef](#)]
67. Oudin, L.; Hervieu, F.; Michel, C.; Perrin, C.; Andréassian, V.; Anctil, F.; Loumagne, C. Which potential evapotranspiration input for a lumped rainfall–runoff model? Part 2—Towards a simple and efficient potential evapotranspiration model for rainfall–runoff modelling. *J. Hydrol.* **2005**, *303*, 290–306. [[CrossRef](#)]
68. Castaneda, L.; Rao, P. Comparison of methods for estimating reference evapotranspiration in Southern California. *J. Environ. Hydrol.* **2005**, *13*, 1–10.
69. Trajkovic, S. Hargreaves versus Penman-Monteith under humid conditions. *J. Irrig. Drain. Eng.* **2007**, *133*, 38–42. [[CrossRef](#)]
70. Ravazzani, G.; Corbari, C.; Morella, S.; Gianoli, P.; Mancini, M. Modified Hargreaves-Samani equation for the assessment of reference evapotranspiration in Alpine river basins. *J. Irrig. Drain. Eng.* **2012**, *138*, 592–599. [[CrossRef](#)]
71. Berti, A.; Tardivo, G.; Chiaudani, A.; Rech, F.; Borin, M. Assessing reference evapotranspiration by the Hargreaves method in north-eastern Italy. *Agric. Water Manag.* **2014**, *140*, 20–25. [[CrossRef](#)]
72. Heydari, M.M.; Heydari, M. Calibration of Hargreaves–Samani equation for estimating reference evapotranspiration in semiarid and arid regions. *Arch. Agron. Soil. Sci.* **2014**, *60*, 695–713. [[CrossRef](#)]
73. Dorji, U.; Olesen, J.E.; Seidenkrantz, M.S. Water balance in the complex mountainous terrain of Bhutan and linkages to land use. *J. Hydrol. Reg. Stud.* **2016**, *7*, 55–68. [[CrossRef](#)]
74. Lobit, P.; López Pérez, L.; Lhomme, J.-P. Retrieving air humidity, global solar radiation, and reference evapotranspiration from daily temperatures: Development and validation of new methods for Mexico. Part II: Radiation. *Theor. Appl. Climatol.* **2018**, *133*, 799–810. [[CrossRef](#)]
75. Althoff, D.; Santos, R.A.d.; Bazame, H.C.; Cunha, F.F.d.; Filgueiras, R. Improvement of Hargreaves–Samani reference evapotranspiration estimates with local calibration. *Water* **2019**, *11*, 2272. [[CrossRef](#)]
76. Romanenko, V. *Computation of the Autumn Soil Moisture Using a Universal Relationship for a Large Area*; Ukrainian Hydrometeorological Research Institute: Kyiv, Ukraine, 1961; pp. 12–25.
77. Schendel, U. Vegetationswasserverbrauch und-wasserbedarf. *Habilit. Kiel.* **1967**, *137*, 1–11.
78. Antal, E. *Új Módszer a Potenciális Evapotranspiráció Számítására*; Beszámoló az 1968-ban Végzett Tudományos Kutatásokról; OMI Hiv. Kiadványa: Budapest, Hungary, 1968; Volume XXXIV, pp. 414–423.
79. Müller, J.; Jörn, P.; Wendling, U. Untersuchungen zur Eignung des ANTAL-Verfahrens für die Bestimmung der potentiellen Evapotranspiration von Gras auf Flachlandstandorten. *Z. Für Meteorol.* **1990**, *40*, 189–191.
80. Linacre, E.T. A simple formula for estimating evaporation rates in various climates, using temperature data alone. *Agric. Meteorol.* **1977**, *18*, 409–424. [[CrossRef](#)]

81. Ahooghalandari, M.; Khiadani, M.; Jahromi, M.E. Developing equations for estimating reference evapotranspiration in Australia. *Water Resour. Manag.* **2016**, *30*, 3815–3828. [[CrossRef](#)]
82. Fox, D.G. Judging air quality model performance: A summary of the AMS workshop on dispersion model performance, woods hole, Mass., 8–11 September 1980. *Bull. Am. Meteorol. Soc.* **1981**, *62*, 599–609. [[CrossRef](#)]
83. Willmott, C.J. On the validation of models. *Phys. Geogr.* **1981**, *2*, 184–194. [[CrossRef](#)]
84. Willmott, C.J. Some comments on the evaluation of model performance. *Bull. Am. Meteorol. Soc.* **1982**, *63*, 1309–1313. [[CrossRef](#)]
85. Willmott, C.J.; Wicks, D.E. An empirical method for the spatial interpolation of monthly precipitation within California. *Phys. Geogr.* **1980**, *1*, 59–73. [[CrossRef](#)]
86. Aschonitis, V.G.; Lekakis, E.; Tziachris, P.; Doulgeris, C.; Papadopoulos, F.; Papadopoulos, A.; Papamichail, D. A ranking system for comparing models' performance combining multiple statistical criteria and scenarios: The case of reference evapotranspiration models. *Environ. Model. Softw.* **2019**, *114*, 98–111. [[CrossRef](#)]
87. Rahimikhoob, H.; Sohrabi, T.; Delshad, M. Assessment of reference evapotranspiration estimation methods in controlled greenhouse conditions. *Irrig. Sci.* **2020**, *38*, 389–400. [[CrossRef](#)]
88. Lang, D.; Zheng, J.; Shi, J.; Liao, F.; Ma, X.; Wang, W.; Chen, X.; Zhang, M. A comparative study of potential evapotranspiration estimation by eight methods with FAO Penman–Monteith method in southwestern China. *Water* **2017**, *9*, 734. [[CrossRef](#)]
89. Valipour, M. Temperature analysis of reference evapotranspiration models. *Meteorol. Appl.* **2015**, *22*, 385–394. [[CrossRef](#)]
90. Trajkovic, S.; Kolakovic, S. Evaluation of reference evapotranspiration equations under humid conditions. *Water Resour. Manag.* **2009**, *23*, 3057–3067. [[CrossRef](#)]
91. Alexandris, S.; Stricevic, R.; Petkovic, S. Comparative analysis of reference evapotranspiration from the surface of rainfed grass in central Serbia, calculated by six empirical methods against the Penman-Monteith formula. *Eur. Water* **2008**, *21*, 17–28.

Disclaimer/Publisher's Note: The statements, opinions and data contained in all publications are solely those of the individual author(s) and contributor(s) and not of MDPI and/or the editor(s). MDPI and/or the editor(s) disclaim responsibility for any injury to people or property resulting from any ideas, methods, instructions or products referred to in the content.